

An Anatomically-Based Model of the Nerves in the Human Foot

Muhammad Zeeshan UIHaque, Peng Du, Leo K. Cheng, Marc D. Jacobs

Abstract—Sensory nerves in the foot play an important part in the diagnosis of various neuropathy disorders, especially in diabetes mellitus. However, a detailed description of the anatomical distribution of the nerves is currently lacking. A computational model of the afferent nerves in the foot may be a useful tool for the study of diabetic neuropathy. In this study, we present the development of an anatomically-based model of various major sensory nerves of the sole and dorsal sides of the foot. In addition, we present an algorithm for generating synthetic somatosensory nerve networks in the big-toe region of a right foot model. The algorithm was based on a modified version of the Monte Carlo algorithm, with the capability of being able to vary the intra-epidermal nerve fiber density in different regions of the foot model. Preliminary results from the combined model show the realistic anatomical structure of the major nerves as well as the smaller somatosensory nerves of the foot. The model may now be developed to investigate the functional outcomes of structural neuropathy in diabetic patients.

Keywords—Diabetic neuropathy, Finite element modeling, Monte Carlo Algorithm, Somatosensory nerve networks

I. INTRODUCTION

THE clinical importance of the nerves of the foot has drawn the attention of clinicians and anatomists. There are various sensory and motor nerves in the dorsal and plantar sides of the foot. The mean epidermal thickness of the skin which covers the dorsum of the foot is approximately 0.064 mm, and underlying the dermis, the hypodermal fat forms a thin layer [1]. The dorsal skin contains the sural nerve, the superficial peroneal nerve and the distal branches of the saphenous nerves, which provide most of the sensory information to the central nervous system; although the terminal branches of the deep peroneal nerve supply the skin over the dorsum of the first web space. The epidermal depth of the plantar skin on the sole of the foot is almost 8 times thicker [1] than that of the dorsal side of the foot. The medial plantar and lateral plantar nerves are the branches of the tibial nerve which supply the sole skin and the intrinsic muscles of the foot. The nerves of the human foot comprise of the combination of unmyelinated and myelinated nerve axons [1], [2], and [23]. These nerves in the foot provide important information about the conduction of sensory action potentials and in the diabetic foot the occurrence of these action potentials is useful in determining diabetic peripheral neuropathy [2], [3].

Numerous studies have been performed on the sensory nerve action potentials based on various techniques, for the diagnosis of diabetic peripheral neuropathy [4] – [9]. These clinical nerve conduction studies can be used to assess both the large myelinated and unmyelinated nerve fiber conductivity. However, intra-epidermal nerve fiber density (IENFD) in skin biopsy is another important measure [8], which is defined as the number of intra-epidermal nerves per unit length of epidermal skin. The intra-epidermal nerve fiber density is comparatively constant throughout life in normal subjects. Yet, epidermal nerve density depends on the anatomical location and a general reduction in epidermal nerve density appears further away from the dorsal root ganglion. There is a decrease in epidermal nerve fiber density observed in diabetic neuropathy at the various anatomic locations [10].

The first finite element model for the motor nerves of the lower limb was made by [11]. They designed an anatomically-based one-dimensional (1D) geometrical model of the posterior motor neurons in the human lower limb to investigate the nerve responses in the lower limb more practically. They used the Chiu, Ritchie, Rogart, Stagg, and Sweeney (CRRSS) [12] electrophysiological model for the action potential propagation in their nerve geometry. They also investigated Functional Electrical Stimulation (FES), a technique which uses a small amount of electrical current to restore the functionality of skeletal muscles that have been paralyzed.

Geometrical modeling of the nerves of the foot offers a tool to recognize the specific nerve damage response for a diabetic foot. To our knowledge, none of the existing geometrical models of the foot has been used specifically in simulating the structural and functional consequences of diabetic neuropathy. For this purpose, we have developed an initial geometrical model of the nerves of the foot.

The main objective of this study was to develop a 1D finite element anatomical model of the major nerves in the sole and dorsal sides of the foot, using known neural topology; along with simplified somatosensory intra-epidermal nerve networks of the foot's skin based on the realistic nerve fiber density at a particular region of the foot. The structure of the somatosensory nerve network is difficult to obtain from empirical histological data for the nerves of the whole foot's skin, due to complexity of dermal and epidermal nerve structures. Therefore, quantitative somatosensory intra-epidermal nerve fiber density data were adapted as a basis for the generation of the somatosensory mesh. For the geometry, many biological structures such as the lung airways, neural structures, blood vessels, and intra-epidermal nerve networks appear as a tree-like bifurcating structure [13], [14].

Muhammad Zeeshan UI Haque, Peng Du, Leo. K. Cheng, and Marc D. Jacobs are with the Auckland Bioengineering Institute, The University of Auckland, New Zealand (phone: +64-9-373-7599; e-mail: mulh001@aucklanduni.ac.nz).

Previously, an improved version of the Monte Carlo method in 3D [15] has been used to generate the bifurcating structures of the airways. This type of geometrical model can now be applied to generate the more distal nerves of the foot. An anatomically-based model of the nerves of the foot would provide a useful platform for simulating the structural and functional aspects of diabetic neuropathy, especially as these occur in conjunction with diabetic foot ulcers.

II. METHODOLOGY

In this study, construction of an anatomically-based 1D model of the major sole and dorsal nerves of the foot together with synthetic somatosensory nerve networks of the foot's skin was fitted in the common continuum mechanics (CM) spatial foot domain which consists of all the bones and muscles modeled in Continuum Mechanics, Image Analysis, Signal Processing and System Identification (CMISS) [16].

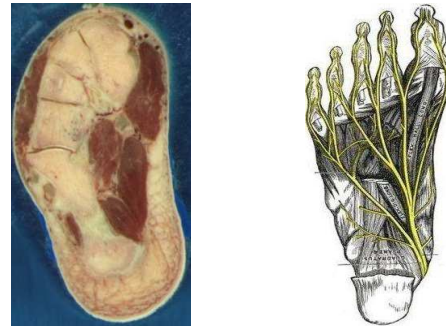
Geometrical modeling of nerves of the foot can be divided into three portions and is described as part of a block diagram in Fig. 1. The details of each of the stages in Fig. 1 are presented in the following sections.

A. Image Digitization in Zinc

The images of the medial and lateral plantar nerves of the foot were obtained from the Visible Human Male (VHM) which has the spatial resolution of 0.33mm in the axial plane and the distance between the slices is 1mm [17]. The images from VHM were manually digitized in the Zinc Digitizer [18] as shown in Fig. 2(a). The resulting data cloud was collected, from which we then identified the estimated position of the medial and lateral plantar digital branches from standard anatomical literature by following the text and illustrations [19].

B. Image Digitization in MATLAB

Since we were unable to see the digital branches of the medial and lateral plantar nerves from VHM, and other major nerves of the foot, potentially due to their small sizes of less than 1mm; we used instead the illustrations of various nerves



(a)

Fig. 2 Image Sources: (a) the Visible Human Male (VHM) [21]; (b) Gray's Anatomy [19]

of the foot from different anatomical studies [19] – [26] as described in Table I. Digitization of these images (e.g., shown in Fig. 2(b)) was completed in MATLAB manually in 2D [27]. Table I shows the various nerves of the foot along with the different anatomical literature and priorities, which we adapted in our neural geometrical model of the foot.

C. Mesh Generation

A mesh was developed from the data points cloud obtained from the manual digitization of VHM images of medial and lateral plantar nerves by using an iterative fitting procedure. The 1D cubic Hermite basis function was used [28] and is given by (1),

$$\mu(\xi) = \Psi_1^0(\xi)\mu^1 + \Psi_1^1(\xi)\left(\frac{\partial\mu}{\partial\xi}\right)^1 + \Psi_2^0(\xi)\mu^2 + \Psi_2^1(\xi)\left(\frac{\partial\mu}{\partial\xi}\right)^2(1)$$

where, “ ξ ” represents the local coordinate with the value lying between 0 and 1 in each direction, “ μ ” represents the value of field at a node, “ Ψ ” defines the cubic Hermite basis function, $\frac{\partial\mu}{\partial\xi}$ refers to the derivative of the field at a given node with respect to the local ξ coordinate, local node numbers are characterized by subscripts of each basis function, and derivative order is characterized by superscript.

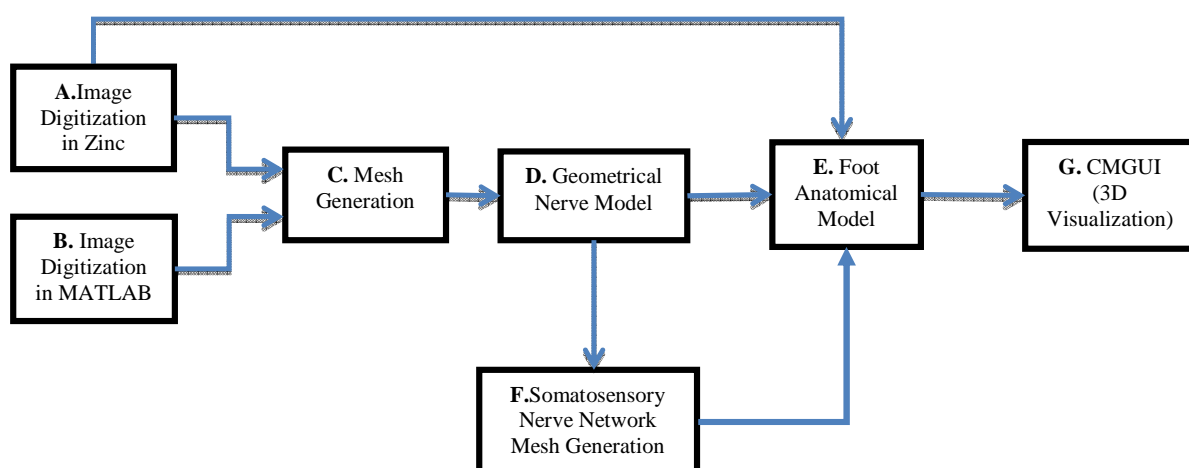


Fig. 1 Block diagram for the geometrical model of the nerves of the foot

An iterative fitting procedure was repeated until the root mean square (RMS) error was minimized to a value of approximately 1 mm. The RMS error for a 1D element is given by (2),

$$RMS\ error = \sqrt{\frac{\sum_{d=1}^D [\mu(\varepsilon_d) - \mu_d]^2}{D}} \quad (2)$$

where, " μ_d " represents the 3-D coordinates of the data points, " $\mu(\varepsilon_d)$ " defines the estimate of finite element field assessed at the ε_d location of the data point, and "D" is the number of data points.

The digitized fine nerve branches were then converted into 3D node points in CMISS by translating and rotating the node points with a scale factor such that it closely registered with the node points obtained from VHM. A series of 1D elements were fitted to the 3D nodepoints. The nodes were chosen to construct a regular mesh with a minimal number of elements required for fitting as described by [28].

D. Geometrical Nerve Model

We fitted both meshes using 1D linear element by estimating the position of the particular nerves of the foot as described in Table I. In this way, generation of the anatomical model of the nerves of the foot could be achieved.

The merged dorsal and plantar nerves of the foot consisted of 380 and 303 elements respectively.

E. Foot Anatomical Model

An anatomically based 3D geometrical model of the right foot was developed based on the VHM dataset. This foot model contained the tricubic Hermite basis elements and fitted to the outer skin layers using the procedure described in [29]. This 3D finite element foot model comprises of all the muscles, bones and an initial model of major nerves of the foot [30], [31].

A host mesh fitting procedure was applied to fit the nerve geometry to the foot model geometry. We adapted the host mesh fitting technique based on a free form deformation (FFD) method and used it to perform geometric transformations on the finite element meshes comprising of rotation, translation, shearing and scaling geometrical operations [29].

The steps which we used to fit the geometrical nerve model in the foot model domain are as follows:

- Initialize the mesh of the geometrical nerve model of the foot in one region.
- Initialize the mesh of the 3D foot model in the other region.
- Translate and rotate the mesh of the geometrical nerve model with optimized scale factor.
- Visualize the nerve mesh to check whether it fitted with the common foot model.
- If not, repeat step 3 until the nerve mesh fit with the 3D foot model.

The surface mesh of the 3D foot model was used as a host mesh in which uniform data points were embedded and the nerve endings were generated by projecting to the external faces of the foot mesh.

The data points on the external faces represented the density of intra-epidermal nerve fiber. This volume mesh served as a volume filling tree of nerve networks. The branch point of the various major dorsal and sole nerves of the foot served as the starting node for the generation of the synthetic somatosensory nerve network of the foot's skin in a specified region.

TABLE I
ANATOMICAL SOURCES FOR MAJOR NERVES

Nerves of the foot	Literature	Priority
Lateral Plantar Nerve (LPN)	William et. al.[19]	++++
- Deep and superficial branches	Moore et. al. [20]	++++
	Birch [21]	++++
- Cutaneous branches	Atlas of Anatomy[22]	+++
- Muscular branches	Arakawa et. al.[23]	+++
- Proper digital branches		
Medial Plantar Nerve (MPN)	William et. al.[29]	++++
- Cutaneous branches	Moore et. al. [20]	++++
- Muscular branches	Birch [21]	++++
- Proper digital nerves of the big toe	Gilroy et. al.[22]	+++
- Proper digital branches		
Medial Calcaneal Nerve (MCN)	William et. al. [19]	++++
	Moore et. al. [20]	+++
	Birch [21]	---
	E. Garner et. al.[24]	+++
Lateral Calcaneal Nerve (LCN)	William et. al.[19]	++++
	Moore et. al. [20]	+++
	Birch [21]	++++
	Gilroy et. al.[22]	++++
Dorsal Cutaneous Nerve (DCN)	William et. al.[19]	++++
	Narendiran et. al. [25]	++++
- Lateral	Moore et. al. [20]	++++
- Intermediate	Birch [21]	+++
- Medial	Gilroy et. al.[22]	+++
Sural Nerve (SN)	William et. al. [19]	++++
	Madhavi et. al. [26]	++++
	Moore et. al. [20]	+++
	Birch [21]	---
	Gilroy et. al.[22]	+++
Saphenous Nerve (SaN)	William et. al. [19]	++++
	Moore et. al. [20]	+++
	Birch [21]	---
	Gilroy et. al.[22]	---
Deep Peroneal Nerve (DPN)	William et. al. [19]	++++
	Moore et. al. [20]	++++
	Birch [21]	+++
	Gilroy et. al.[22]	+++

"++++" indicates frequently implemented/used in the model.

"+++" indicates infrequently implemented in the model.

"---" indicates not used in the model.

TABLE II
PARAMETERS FOR THE GENERATION OF SYNTHETIC INTRA-EPIDERMAL NERVE BIFURCATING TREE

PARAMETERS	VALUES
Branching angle limit	60°
Length limit	1.2 mm
Branching fraction	0.4
Total no. of faces in toe's skin	19

F. Somatosensory Nerve Network Mesh Generation

An algorithm was needed which automatically generates the intra-epidermal nerve structures of the skin. Wang [32] previously has developed an algorithm which grows biological structures in the form of bifurcation in a defined region in 2D space and it is based on the Monte Carlo method.

A modified version of the Monte Carlo method in 3D [15] was used to generate bifurcating somatosensory intra-epidermal nerve structures in the big toe. This tree generation is described in Fig. 3 in the form of a simple cube. This 3D algorithm was chosen because of its comparative simplicity, hence it was computationally cheaper to implement in 3D in the defined region of interest.

This algorithm worked as follows:

- Determine the center of mass of the points in a specified region by averaging the individual co-ordinate positions in Fig. 3(a).
- A splitting plane is used to cover the host borders. Two subcollections of points are designated on either side of the plane shown in Fig. 3(b).
- Calculate the center of mass of every subcollection of points as depicted in Fig. 3(c).
- At the end of the current branch, a branch is generated for every subcollection of points as presented in Fig 3(d).
- Calculate the branch angle which is the angle between the parent branch and the newly generated branch. The angle is reduced if it is larger than the defined angle limit.
- Calculate the branch length. A check is performed for the branch length. When the branch length is equal to the length limit or approaches within the length limit of the host volume mesh, then the branch is terminated; in certain cases where the growing branch extends beyond the host volume mesh, its length is decreased until the last point lies on the host volume mesh.
- Reallocate data points for the completion of all branching for a single generation. This progression is repeated until all the pathways are terminated by a terminal branch at the external face of the foot volume mesh.

III. RESULTS AND DISCUSSION

The anatomically-based geometrical model of the major nerves of the foot is depicted in Fig. 4. The model consists of five major dorsal nerves and three major plantar nerves. In addition, we have also depicted 26 bones and 20 muscles in this foot model, in order to demonstrate the spatial orientations of the major nerve branches relative to these tissue structures. The foot's skin surface is represented by the tissue color, nerves are represented by the green lines, bones are represented by white surfaces and muscles represented by red surfaces, respectively.

Here we also present an initial bifurcating intra-epidermal nerve network at the big toe of the right foot. The intra-epidermal nerve fiber density represents the ratio of epidermal nerve endings per mm of length and was used in our designed geometry. Here, we assumed the intra-epidermal nerve fiber density is 20 nerve endings/mm of epidermal length, based on reported experimental data [33], which implies 400 nerve endings/mm².

Based on a big toe surface area of 3281.83 mm² and 400 nerve endings/mm², the estimated total number of nerve endings was 1,312,732. Building a comprehensive model with a realistic number of nerve terminals in the whole foot proved computationally demanding. Therefore, we scaled the density of nerve endings by a factor of 100, which resulted in a total of 13,127 nerve endings. The branching fraction of 0.4 (Table II) was selected because the average branch angle then approached the theoretical ideal angle of the biological structure [34]. The range of branching angle of the biological neuronal structure can generally vary from 58° to 62° [35], [36]. Hence, the branching angle limit of 60° was implemented in the bifurcated nerve geometrical model.

Various views of the generated synthetic somatosensory intra-epidermal nerve network at the big toe are presented in Fig. 5. This figure shows bifurcating trees which were generated from the proper digital nerves of the various dorsal and plantar nerves of the foot. The bifurcating trees were joined together in a single synthetic nerve network of the skin of the big toe. This somatosensory nerve network is represented by red color, along with the various dorsal and plantar nerves, which are represented by green color.

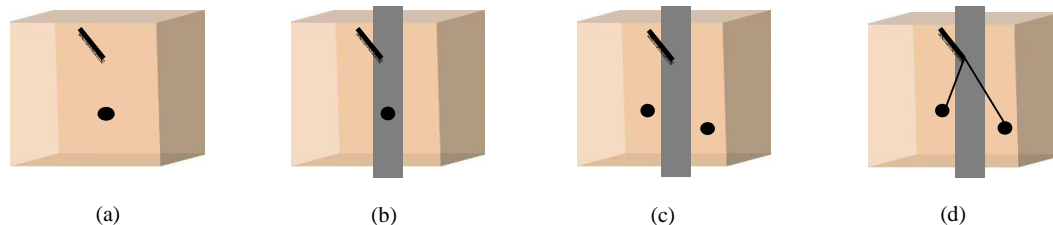


Fig. 3 Modified illustration of 3D tree growing algorithm in a simple cube [15]: (a) center of mass of uniform points is determined (black dot); (b) splitting plane is defined; (c) the center of mass of every subcollection of points is calculated; (d) branches are generated from each of the major nerves and subcollection centers of mass

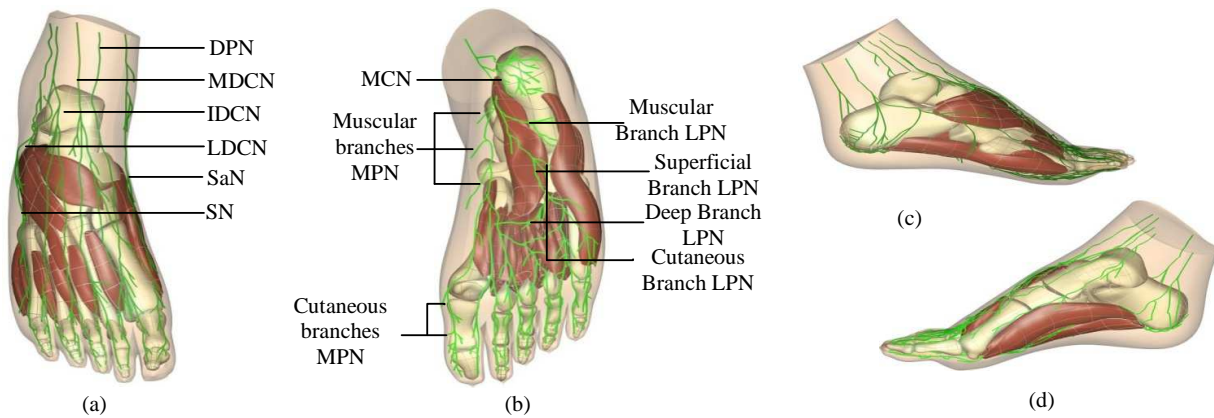


Fig. 4 Geometrical model of the nerves of the foot: a) various major dorsal nerves of the foot; b) various major plantar nerves; c) lateral view of the nerves of the foot; d) medial view of the nerves of the foot. For abbreviations see Table I

IV. CONCLUSION AND FUTURE WORKS

This paper described the development of an anatomically-based geometrical model of the major nerves in the dorsal and plantar sides of the foot, using various anatomical literatures. We also developed a model of the somatosensory intra-epidermal nerve networks at the big toe based on the realistic nerve fiber density. In the future, the nerve generating algorithm will be applied to spread the somatosensory intra-epidermal nerve network throughout the skin of the whole foot. Once this task is accomplished, then this type of geometrical model of the nerves of the foot can provide a useful platform for simulating the structural and functional aspects of diabetic neuropathy in the foot.

ACKNOWLEDGMENT

The first author would like to acknowledge the New Economy Research Fund (NERF) of New Zealand. The first author would also thank Dr. Justin Fernandez and Associate Professor Merryn Tawhai for providing support in the development of this nerve model of the foot.

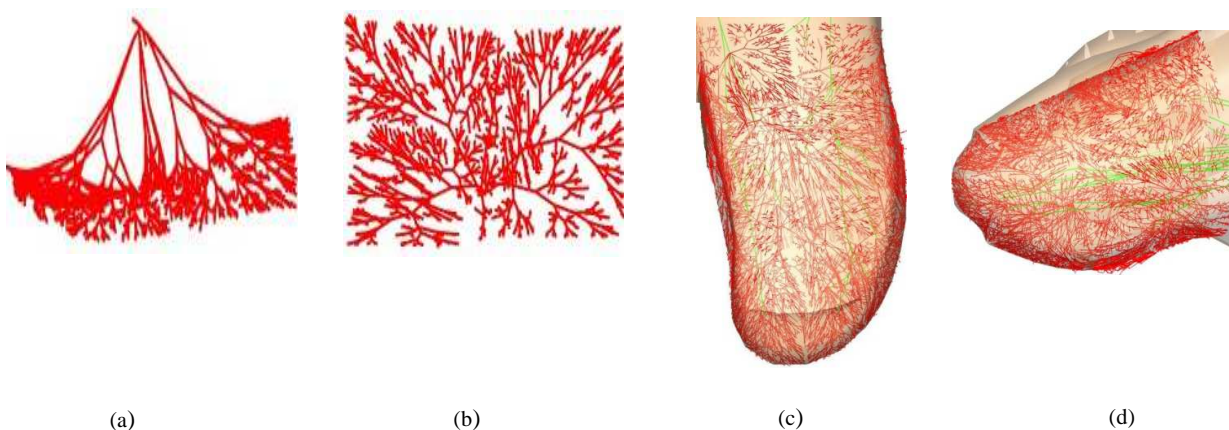


Fig. 5 Various views of synthetic bifurcated somatosensory intra-epidermal nerve network: (a) tree generation; (b) front view; (c) generated bifurcated tree at the big toe surface of the foot's skin; (d) bifurcated tree with view of the plantar nerves.

REFERENCES

- [1] S. Bianchi, and C. Martiloni, "Foot," *Ultrasound of Musculoskeletal System*, Springer Verlag, pp.835-850, 2007.
- [2] J. Craven, "Nerves of the leg and foot," *Anaesthesia and Intensive Care Medicine*, Vol. 8:4, pp. 149-150, 2007.
- [3] S. Grimnes, and O. J. Martinsen, *Excitable tissues and Bioelectric Signal: Bio impedance and Bioelectricity Basics*, San Diego, Calif., London: Academic. 2000, pp. 139- 159.
- [4] C. Sylantiev, R. Schwartz, J. Chapman, and A. S. Buchman, "Medial Plantar Nerve Testing Facilities Identification of Polyneuropathy," *Muscle and Nerve* Vol. 38, pp. 1595-1598, 2008.
- [5] J. Y. An, M. S. Park, J. S. Kim, Y. M. Shon, S. J. Lee, Y. I. Kim, K. S. Lee, and B. J. Kim, "Comparison of Diabetic Neuropathy Symptom Score and Medial Plantar Sensory Nerve Conduction Studies in Diabetic Patients showing Normal Routine Nerve Conduction Studies," *International Medicine* Vol. 47, 1395-1398, 2008
- [6] S. J. Oh, K. W. Lee, J. S. Hah, D. E. Kim, M. Demirci, "Lateral Plantar Neuropathy," *Muscle and Nerve*, Vol. 22, pp. 1234-1238, 1999.
- [7] S. J. Oh, H. S. Kim, and B. K. Ahmad, "Electrophysiological Diagnosis of Inter-digital Neuropathy of the foot," *Muscle and Nerve*, Vol. 7, pp. 218-225, 1984.
- [8] S. H. Horowitz and C. Krarup C, "Conduction studies of the normal sural nerve," *Muscle and Nerve*, Vol. 15, pp. 374-383, 1992.
- [9] S. J. Oh, M. Demirci, B. Dajani, A. C. Melo, and G. C. Claussen, "Distal Sensory Nerve Conduction of the Superficial Peroneal Nerve: New Method and its Clinical application," *Muscle and Nerve*, Vol. 24, pp. 689-694, 2001.
- [10] B. Bakotic, "Epidermal Nerve fiber density: an overview," *Podiatry management*, pp. 141- 152, 2010.
- [11] J. Kim, J. Davidson, O. Rohrl, T. Soboleva, and A. Pullan, "Anatomically based lower limb model for electrical stimulation," *Biomedical Engineering online*, Vol. 6:48, 2007.
- [12] S. Chiu, J. Ritchie, R. Rogart, D. Stagg, and Sweeney, "A quantitative description of membrane currents in rabbit myelinated nerve," *The Journal of Physiology*, Vol. 292, pp. 149-166, 1979.
- [13] H. C. Yeh, "Modeling of Biological Structure," *Bulletin of Mathematical Modeling*, vol. 41, pp. 893-898, 1979.
- [14] V. Olsbo, and L. Waller, "A point process approach to modeling epidermal nerves fiber patterns," *Technical report 08-03*, pp. 1-20, 2008.
- [15] M. H. Tawhai, A. J. Pullan, and P. J. Hunter, "Generation of an anatomically based three dimensional model of the conducting airways," *Annals of Biomedical Engineering*, Vol. 28, pp. 793-802, 2000.
- [16] CMISS: <http://www.cmiss.org>.
- [17] V. Spitzer, M. Ackerman, A. Scherzinger, and D. Whitlock, "The Visible Human Male: a technical report," *Journal of American Medical Informatics Ass* Vol. 3, No. 2, pp. 118-130, 1996.
- [18] Zinc Digitizer: <http://www.cmiss.org/cmgui/zinc>.
- [19] P. L. William, R. Warwick, M. Dyson, and L. H. Bannister, "Neurology: The Tibial Nerve," *The Gray's Anatomy*, 37 Editions, pp. 1142 – 1149, 1989.
- [20] K. L. Moore, A. M. Ragur, and A. F. Dalley, "Lower Limb," *Clinically oriented anatomy*, Edition 6, pp. 614-618, 2011.
- [21] R. Birch, "The peripheral Nervous system: Gross Anatomy," *Surgical disorders of the peripheral nerves*. Springer-verlag London limited, pp. 1-41, 2011.
- [22] J. A. Gilroy, B. R. MacPhason, L. M. Roses, "Ankle and foot," *Atlas of Anatomy*, Stuttgart; New York: Thieme, pp. 432-445, 2008.
- [23] T. Arakawaa, S. Sekiyab, K. Kumakic, and T. Terashimaa, "Ramification pattern of the deep branch of the lateral plantar nerve in the human foot," *Annals of Anatomy*, Vol. 187(3):287-96, 2005.
- [24] E. Garner, and D. J. Gray, "The innervation of the joint of the foot," *The Anatomical Record*, Vol. 161 (2), pp. 141-148, 1968.
- [25] N. K. Narendiran, R. K. G. Mohandas, S. N. Somayaji and V. Rodriques, "Clinically important anatomical variation of cutaneous branches of superficial peroneal nerve in the foot," *The open anatomy journal*, Vol. 2, pp 1-4, 2010.
- [26] C. Madhavi, B. Isaac, B. Antoniswamy, and S. J. Holla, "Anatomical variations of the cutaneous innervation patterns of the sural nerve on the dorsum of the foot," *Clinical anatomy*, Vol. 18, pp. 206-209, 2005.
- [27] MATHWORKS: <http://www.mathworks.com/products/matlab/>.
- [28] C. Bradley, A. Pullan, and P. Hunter, (1997). "Geometric Modeling of the Human Torso," *Annals of Biomedical Engineering*, Vol. 27(1), pp. 96-111, 1997.
- [29] J. W. Fernandez, K. Mithraratne, S. F. Thrupp, M. H. Tawhai, and P. Hunter, "Anatomically based geometric modelling of the musculoskeletal system and other organs," *Biomechanics and Modeling in Mechanobiology*, Vol. 2(3), pp.139-155, 2004.
- [30] J. W. Fernandez, J. Jor, M. Z. Ul Haque, M. D. Jacobs, P. J. Hunter, and K. Mithraratne, "Nerve excitation in the diabetic foot: An anatomically based model to explore external therapies for mechano-stimulation of sensory nerves," *Proceedings of the 23rd Congress of the International Society of Biomechanics*, Brussels, 3-7 July 2011.
- [31] J. W. Fernandez, M. Z. Ul Haque, P. J. Hunter, and K. Mithraratne, "Mechanics of the foot – Part 1: Part 1: A continuum framework for evaluating soft tissue stiffening in the pathologic foot," in *International Journal for Numerical Methods in Biomedical Engineering*; (in press).
- [32] C. Y. Wang, J. B. Bassingthwaite, and L. J. Weissman, "Bifurcating distributive system using Monte Carlo method," *Math. Computational modeling*, Vol.16 (3), pp. 91-98, 1992.
- [33] M. C. Ferreira, S. A. T. Vieira, and V. F. D. Carvalho, "Comparative study of the sensitivity of diabetic lower extremities with and without ulcers using the PSSDTM," *Acta Ortop Bras*, Vol. 18(2), pp. 71-4, 2010.
- [34] K. Horsfield, and G. Cumming, "Angles of branching and diameters of branches in the human bronchial tree," *Bulletin Math. Biophysics*, Vol. 29, pp. 245-259, 1967.
- [35] O. Shefi, A. Harel, D. B. Chklovskii, E. B. Jacobs, and A. Ayali, "Biophysical constraints on neural branching," *Neurocomputing*, Vol. 58(60), pp. 487-495, 2004.
- [36] O. Shefi, S. Golebowicz, E. B. Jacobs, and A. Ayali, "A two phase growth strategy in cultured neural networks as reflected by the distribution of neurite branching angles," *Inc. J Neurobiol*, Vol. 62, pp. 361-368, 2005.